AFRL-RD-PS-
TP-2010-1010

THE AGGREGATE BEHAVIOR OF BRANCH POINTS- BRANCH POINT DENSITY AS A CHARACTERISTIC OF AN ATMOSPHERIC TURBULENCE SIMULATOR (POSTPRINT)

Denis Oesh et al.

Air Force Research Laboratory
3550 Aberdeen Ave SE
Kirtland AFB, NM 87117

1 June 2009

Technical Paper

AIR FORCE RESEARCH LABORATORY
Directed Energy Directorate
3550 Aberdeen Ave SE
AIR FORCE MATERIEL COMMAND
KIRTLAND AIR FORCE BASE, NM 87117-5776

REPORT DOCUMENTATION PAGE

Form Approved
OMB No. 0704-0188

1. REPORT DATE *(DD-MM-YYYY)*	2. REPORT TYPE	3. DATES COVERED *(From - To)*
01-06-2009	Technical Paper	June 1, 2009 - October 1, 2009

4. TITLE AND SUBTITLE
The Aggregate Behavior of Branch Points- Branch Point Density
As a Characteristic of an Atmospheric Turbulence Simulator (Post print)

5a. CONTRACT NUMBER
In House DF702151

5b. GRANT NUMBER

5c. PROGRAM ELEMENT NUMBER
62890F

6. AUTHOR(S)
*Denis W. Oesch, Darryl J. Sanchez, Carolyn M Tewksbury-Christle, Patrick R. Kelly

5d. PROJECT NUMBER
2301

5e. TASK NUMBER
SJ

5f. WORK UNIT NUMBER
41

7. PERFORMING ORGANIZATION NAME(S) AND ADDRESS(ES)

AFRL/RDSA
3550 Aberdeen Ave SE
Kirtland AFB, NM 87117-5776

*Science Applications International Corp.
2109 Airpark Road SE
Albuquerque, NM 87106

8. PERFORMING ORGANIZATION REPORT NUMBER

9. SPONSORING / MONITORING AGENCY NAME(S) AND ADDRESS(ES)
Air Force Research Laboratory
3550 Aberdeen Ave SE
Kirtland AFB, NM 87117

10. SPONSOR/MONITOR'S ACRONYM(S)
AFRL/RDSAE

11. SPONSOR/MONITOR'S REPORT NUMBER(S)
AFRL-RD-PS-TP-2010-1010

12. DISTRIBUTION / AVAILABILITY STATEMENT
Approved for Public Release

13. SUPPLEMENTARY NOTES
Accepted for publication at the SPIE Annual Conference; San Diego, CA; August 6, 2009. 377ABW-2009-1028; August 5, 2009. "Government Purpose Rights"

14. ABSTRACT
The atmospheric turbulence simulator used in testing in the atmospheric simulation and adaptive-optic laboratory test-bed at Starfire Optical Range is configured based on three characteristics: Fried's parameter, the Rytov number and the Greenwood Frequency. All three may be estimated from open loop data as a means of verifying the simulated turbulence conditions for a given test configuration. However, unlike Fried's parameter and the Greenwood Frequency the Rytov number isn't directly calculated. Instead the scintillation index is estimated from intensity measurements. At low Rytov values, (<0.3-0.4), this measurement can approximate the Rytov number; however beyond a Rytov of 0.4 this parameter becomes saturated. Branch Points begin to appear after the Rytov value exceeds 0.1. In this work the behavior of branch point density is examined to determine its viability as another parameter for calibration our turbulence simulator.

15. SUBJECT TERMS
Branch points; density; atmospheric; turbulence; adaptive optics

16. SECURITY CLASSIFICATION OF:			17. LIMITATION OF ABSTRACT	18. NUMBER OF PAGES	19a. NAME OF RESPONSIBLE PERSON
a. REPORT	b. ABSTRACT	c. THIS PAGE	SAR	14	Patrick Kelly
Unclassified	Unclassified	Unclassified			19b. TELEPHONE NUMBER *(include area code)* 505-846-2094

Standard Form 298 (Rev. 8-98)
Prescribed by ANSI Std. 239.18

This page is intentionally left blank.

The Aggregate Behavior of Branch Points - Branch Point Density as a Characteristic of an Atmospheric Turbulence Simulator

Denis W. Oesch[a], Darryl J. Sanchez[a], Carolyn M. Tewksbury-Christle[a], Patrick R. Kelly[a]

[a]Starfire Optical Range, Air Force Research Labs, Kirtland Air Force Base, New Mexico, USA

ABSTRACT

The Atmospheric Turbulence Simulator used in testing in the Atmospheric Simulation and Adaptive-optic Laboratory Test-bed at Starfire Optical Range is configured based on three characteristics: Fried's parameter, r_0, the Rytov number, σ_χ^2, and the Greenwood Frequency, f_G. All three may be estimated from open loop data as a means of verifying the simulated turbulence conditions for a given test configuration. However, unlike r_0 and f_G, the Rytov number isn't directly calculated. Instead the scintillation index is estimated from intensity measurements. At low Rytov values, ($< 0.3 - 0.4$), this measurement can approximate the Rytov number, however beyond a Rytov of 0.4 this parameter becomes saturated. Branch Points begin to appear after the Rytov value exceeds 0.1. In this work the behavior of the branch point density is examined to determine its viability as another parameter for calibration our turbulence simulator.

Keywords: branch points, density, atmosphere, turbulence, adaptive optics

1. INTRODUCTION

To calibrate our experimental conditions in the Atmospheric Simulation and Adaptive-optic Laboratory Testbed (ASALT) at Starfire Optical Range, it is standard practice to collect open loop data during experiments for each Atmospheric Turbulence Simulator (ATS)[1] configuration under which closed loop data is collected. This open loop data provides an independent verification that the tests were conducted under the prescribed conditions. Processing of this data provides measurements of Fried's parameter, r_0, the Greenwood Frequency, f_G, and the scintillation index.

The scintillation index is approximately equivalent to the Rytov parameter for values of the Rytov $< 0.3 - 0.4$. It is well known from experimental data that at Rytov ≈ 0.1 branch points begin to appear in the data. It was suggested that branch point density might be used as an alternative to the scintillation index for calibrating the configuration of the ATS. The purpose of this work was to examine the functional dependencies of the branch point density on other system parameters to determine it's use as a calibration parameter.

2. BACKGROUND

The ASALT laboratory is uniquely suited to studying the saturation regime, Rytov > 0.4. The laboratories have 3 full bench top adaptive optic systems each with its own ATS and multiple deformable mirror (DM) - wavefront sensor (WFS) pairs, all operating at 1.55 μm. For this work the WFS was a temporal SRI with 256x256 pixel resolution over a simulated 1.5 m aperture. The ATS consists of two 6 inch phase screens etched with a Kolmogorov structure function set in converging beam space providing for a range of turbulence conditions. By varying the position of each phase wheel along a rail provides a method for adjusting r_0 between roughly 4 and 30 cm while also varying Rytov from 0 up to roughly 2.4. Stepper motors control the rate of rotation of the phase wheels and allow for selectable Greenwood Frequencies, f_G. The wheels are fitted with a hardware home that provides repeatability of turbulence conditions over multiple tests. To this standard ATS set-up an optical trombone was added between the low altitude phase wheel and the system pupil to provide for a variable free space propagation.

Further author information: (Send correspondence to Denis W Oesch)
E-mail: denis.w.oesch@saic.com

The optical trombone allows partial decoupling of the r_0 and Rytov parameters. Thus providing a means of varying the distance to the turbulence layer and hence the Rytov parameter, while maintaining a constant turbulence strength. This made isolating the contributions to the distribution of branch points seen in the pupil plane from turbulence strength and distance independently. Leading to an understanding of how the configuration of the phase wheels relates to the measured branch point densities.

There has been significant work on branch points in atmospheric turbulence and their impact on adaptive optics systems[2–13] and even one specifically on branch point density.[14] However these hasn't been an experimental test of this type that we have found in the literature which allows for the isolation of the turbulence strength and the propagation distance as has been done in this work.

3. PROBLEM FORMULATION

The Rytov approximation forms the theoretical basis of adaptive optics.[15] With this approximation and a Kolmogorov structure function, it has been shown[15,16] that four moments of the atmospheric structure function determine AO performance, the zeroth altitude moment, r_0, the $(5/6)^{\text{th}}$ altitude moment, σ_χ^2, the $(5/3)^{\text{th}}$ altitude moment, θ_0, and the $(5/3)^{\text{th}}$ velocity moment, f_G. We generate these parameters using our atmospheric turbulence simulator (ATS).

Our ATS consists of two turbulence layers each with adjustable strengths and altitudes. In its standard configuration, r_0 and σ_χ^2 are coupled because both are functions of ATS phase wheel position (and phase wheel position Fresnel scales to altitude). To partially mitigate the coupling of these parameters, an optical trombone was added in collimated space after the second (low altitude) phase wheel. This allows for an increase in propagation distance without changing the atmospheric structure function and this allows variation of σ_χ^2 without changing r_0, i.e. the altitude of the phase screens can be displaced by ΔL causing $z_{\text{low}} \rightarrow z_{\text{low}} + \Delta L$ and $z_{\text{high}} \rightarrow z_{\text{high}} + \Delta L$. So, with $C^2_{n,\text{low}}$ and $C_{n,\text{high}}$ denoting the low and high altitude structure functions, respectively. Then,

$$C_n^2(z) = C^2_{n,\text{low}}(z)\delta(z - z_{\text{low}}) + C^2_{n,\text{high}}(z)\delta(z - z_{\text{high}}) \tag{1}$$

which causes the no trombone version of the Rytov parameter,

$$\sigma_\chi^2 = 0.291 k_0^{7/6} \int_0^L C_n^2(z)(\gamma z)^{5/6}\, dz$$

to go to

$$\begin{aligned} \{\sigma_\chi^2\}_{\text{with trombone}} &= 0.291 k_0^{7/6} \textstyle\int_0^{L+\Delta L} C_n^2(z)(\gamma z)^{5/6}\, dz \\ &= 0.291 k_0^{7/6} \left(C^2_{n,\text{low}}(z_{\text{low}})(\gamma(z_{\text{low}} + \Delta L))^{5/6} + C^2_{n,\text{high}}(z_{\text{high}})(\gamma(z_{\text{high}} + \Delta L))^{5/6} \right) \\ &\neq \{\sigma_\chi^2\}_{\text{no trombone}} \end{aligned} \tag{2}$$

but the no trombone version of the Fried parameter,

$$r_0 = \left(0.423 k_0^2 \int_0^L C_n^2(z)\, dz \right)^{-3/5}$$

goes to

$$\begin{aligned} \{r_0\}_{\text{with trombone}} &= \left(0.423 k_0^2 \textstyle\int_0^{L+\Delta L} C_n^2(z)\, dz \right)^{-3/5} \\ &= \left(0.423 k_0^2 \left(C^2_{n,\text{low}}(z_{\text{low}}) + C^2_{n,\text{high}}(z_{\text{high}}) \right) \right)^{-3/5} \\ &= \{r_0\}_{\text{no trombone}} \end{aligned} \tag{3}$$

where $\gamma = 1$ for a plane wave, k_0 the wave number, L either the distance to the guide star or the top of the atmosphere, and C_n^2 the atmospheric structure function. This is equivalent to the electromagnetic field encountering turbulence followed by a free space propagation of variable length. The separation of the turbulence layer and the pupil can be adjusted which changes the Rytov parameter and, in-turn, alters the number of branch points in the pupil.

3.1 Definition of a Branch Point

A branch point is a zero of an analytic function. Following Fried,[3,8] let $w(x,y)$ be the scalar function representing an optical field and let $u(x,y)$ and $v(x,y)$ be the real and imaginary parts of that function, respectively, then

$$w(x,y) = u(x,y) + iv(x,y). \tag{4}$$

where the amplitude, $A(x,y)$, and phase, $\phi(x,y)$, of this field will be given by

$$A(x,y) = \sqrt{u^2(x,y) + v^2(x,y)} \tag{5}$$

and

$$\phi(x,y) = arg(w(x,y)) + 2\pi\kappa. \tag{6}$$

Where $\kappa = \kappa(x,y)$ are two-dimensional step functions of height 2π.

From the theory of analytic functions, a branch point at (x_p, y_p) is equivalent to both

$$w(x_p, y_p) = 0 \tag{7}$$

and

$$\int_{C'} d\vec{l}' \cdot \vec{\nabla}_\phi(x', y') = \pm 2\pi \tag{8}$$

for C' a closed curve encircling the one branch point at (x_p, y_p). and $\vec{\nabla}_\phi$ the gradient operator acting on ϕ. Also, for discussional clarity, we call $sign\left(\int_{C'} d\vec{l}' \cdot \vec{\nabla}_\phi(x', y') = \pm 2\pi\right)$ the polarity of the branch point.

3.2 Identification of a Branch Point's Position and Polarity in Experimental Data

Experimentally, the analytic function is sampled, such that the measurement is an average over a detector pixel. Therefore, the theoretical expressions given in Equations 7 and 8 must be modified such that given a branch point at (x_p, y_p) and pixels centered at $P_A := (x_A, y_A)$, $P_B := (x_A + \Delta X, y_A)$, $P_C := (x_A + \Delta X, y_A - \Delta Y)$, and $P_D := (x_A, y_A - \Delta Y)$ such that $x_A < x_p < x_A + \Delta X$ and $y_A < y_p < y_A + \Delta Y$ then

$$w_m(x_p, y_p) \neq 0 \tag{9}$$

where w_m is the measured value of the scalar function, $w(x_p, y_p)$. Hence, an experimental measurement of the zero crossings of $w(x,y)$ cannot be used to determine the location of branch points. On the other hand, the circulation in phase given by the integral in Equation 8, $\int_{C'} d\vec{l}' \cdot \vec{\nabla}_\phi(x', y')$, when sampled, goes to

$$(\phi(P_B) - \phi(P_A)) + (\phi(P_D) - \phi(P_B)) + (\phi(P_C) - \phi(P_D)) + (\phi(P_A) - \phi(P_C)) \tag{10}$$

with the contour C' given by

$$C' : (P_A) \rightarrow (P_B) \rightarrow (P_D) \rightarrow (P_C) \rightarrow (P_A), \tag{11}$$

(see Figure 1). Equation 10 still measures the $\pm 2\pi$ circulation in phase indicative of branch points, and hence, this expression is used to find branch points in experimental data. To implement this, we sum the gradients of the phase around a closed loop in the 2π modulo phase, with all loops chosen to be elementary circulations, i.e. a $2x2$ region of the 2π modulo phase was used for each loop. If the sum of the phase gradients is $\pm 2\pi$, an odd number of branch points exists within the loop. We assume that there is only one branch point within the loop. We then assign the location of the branch point as the intersection of the four pixels with its polarity given by the sign of the circulation. This is a standard technique for isolating branch points from phase data.[3]

4. BRANCH POINT DENSITY

The density of the branch points should increase with propagation distance and provide additional information in characterizing the profile of the atmospheric turbulence. To determine the relative influence of the distance and strength of the turbulence, open loop data was compiled with the temporal SRI. The data collected from this camera was processed for branch point density in a range of configurations.

4.1 Data and Methodology

For these test sequences, a single phase wheel was used in conjunction with the optical trombone described in Section ??. In each data run, the strength of the turbulence is maintained while the distance to the turbulence layer is increased. This increase takes the form of eleven evenly spaced steps over a roughly 9 km range, providing a test region from 0 - 15 km. This independently varies the Rytov parameter from $0 - 1.2$ as shown in Figure 2. Between each data run, the turbulence strength, which in our test-bed is equivalent to varying r_0, is modified. In this way, eleven values of atmospheric strength were interrogated, ranging from 6.52 to 16.60 cm. See Table 1. For each trombone position and turbulence strength the phase wheel was rotated at a constant speed for 200 frames. Data was collected for each configuration producing $200 - 256x256$ images of the phase for each of 121 turbulence conditions.

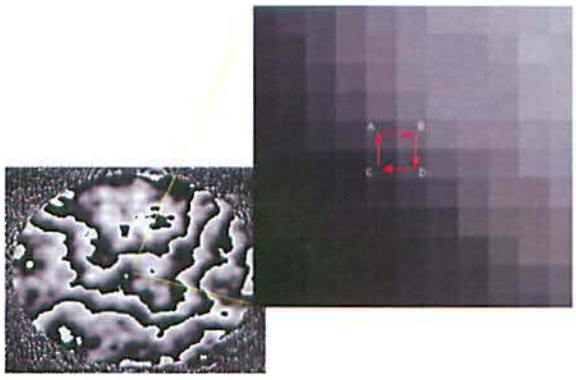

Figure 1. *Sample 2π modulo phase with enlarged portion showing an example of an elementary circulation.*

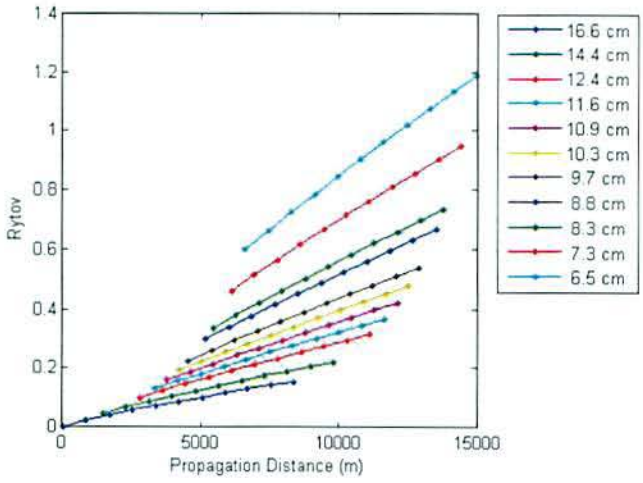

Figure 2. *Theoretical Rytov values for the single phase wheel test configurations as displayed in Table 1. Each curve is representative of the predicted Rytov number for a series of trombone positions, $0 - 50$ cm through a constant turbulence strength. Here represented as a constant r_0 as indicated in the legend. All values are computed for a simulated 1.5 meter aperture.*

4.2 Measured Density

The density of the branch points is easily calculated by simply applying the techniques in Section 3.2 to find the branch points, then averaging the number of branch points over all frames collected and dividing by the area of the aperture. This is done for each of the 121 configurations given in Table 1. For each of the data sets, Figure 3 plots branch point density along the vertical axis versus propagation distance on the horizontal axis. Each curve represents a different turbulence strength denoted by the legend. Via Equation 3, turbulence strength is given

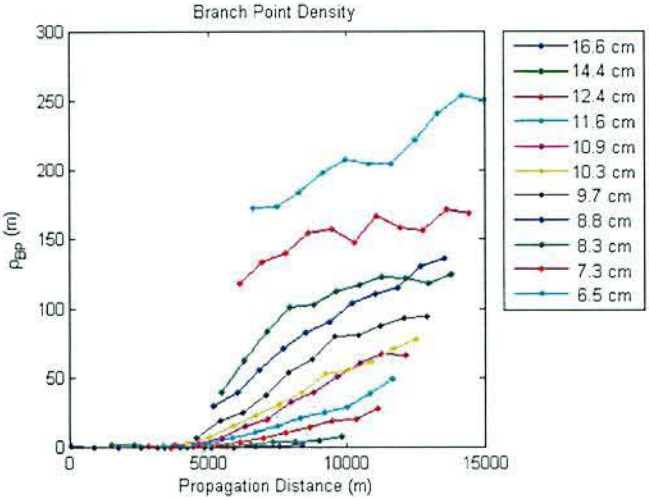

Figure 3. *Branch point density from single phase wheel data for selected turbulence strengths. For each curve, the turbulence strength, given by r_0, is held constant while the propagation distance is varied using the optical trombone. Raw branch point density vs propagation distance.*

as r_0 in centimeters in output space assuming a $1.5m$ pupil.

As can be seen, the branch point density increases with propagation distance. It also increases with turbulence strength. Of the two, there is a stronger dependence on turbulence strength than propagation distance.

4.3 Transforming by z_0

The curves presented in Figure 3 appear to shift to the left as the strength of the turbulence increases. Implying that there may be some minimum distance, z_0 under which branch points simply won't form for a given turbulence

			ATS Configuration			Turbulence Conditions			
Ensemble Set #	Number of Realizations	Lens Set	Trombone Position (cm)	PW Position (low, high) (cm)	PW Step (low, high) (counts)	Propagation Range (km)	Turb. Velocity (low, high) (m/s)	r_0 (cm)	σ_χ^2
1	200	7	{0:5:50}	(106.3, 55.5)	(3, 0)	0.0-8.4	(11.75, 0)	16.6	0.00 – 0.15
2	200	7	{0:5:50}	(105.5, 55.5)	(3, 0)	1.5-9.8	(10.22, 0)	14.4	0.04 – 0.22
3	200	7	{0:5:50}	(104.5, 55.5)	(3, 0)	2.8-11.1	(8.79, 0)	12.4	0.10 – 0.32
4	200	7	{0:5:50}	(104.0, 55.5)	(3, 0)	3.3-11.7	(8.22, 0)	11.6	0.13 – 0.37
5	200	7	{0:5:50}	(103.5, 55.5)	(3, 0)	3.8-12.1	(7.71, 0)	10.9	0.16 – 0.42
6	200	7	{0:5:50}	(103.0, 55.5)	(3, 0)	4.2-12.6	(7.27, 0)	10.3	0.19 – 0.48
7	200	7	{0:5:50}	(102.5, 55.5)	(3, 0)	4.6-12.9	(6.87, 0)	9.7	0.23 – 0.54
8	200	7	{0:5:50}	(101.5, 55.5)	(3, 0)	5.2-13.5	(6.20, 0)	8.8	0.30 – 0.67
9	200	7	{0:5:50}	(101.0, 55.5)	(3, 0)	5.4-13.8	(5.91, 0)	8.3	0.34 – 0.73
10	200	7	{0:5:50}	(99.5, 55.5)	(3, 0)	6.1-14.4	(5.18, 0)	7.3	0.46 – 0.95
11	200	7	{0:5:50}	(98.0, 55.5)	(3, 0)	6.6-15.0	(4.61, 0)	6.5	0.60 – 1.19

Table 1. *Turbulence parameters used for measurement of branch point density and separation. For each Ensemble set, 200 frames of data was collected for each of 11 positions of the optical trombone, ranging in 5 cm increments from 0 to 50 cm. This corresponds to ranges of propagation distances and Rytov parameters for each Ensemble.*

strength. From experimental results, the first branch points form when $\sigma_\chi^2 \approx 0.1$. Evaluating Equation 2, for a single turbulence layer produces the relationship

$$\sigma_\chi^2 = 0.5631(\frac{6.88}{2.91})k_0^{-5/6} r_0^{-5/3} z_0^{5/6}. \tag{12}$$

Setting $\sigma_\chi^2 = 0.1$ and solving for z, allows Equation 12 to be transformed into an equivalent distance, z_0

$$z_0 = 0.0448 k_0 r_0^2. \tag{13}$$

which can be considered the theoretical value at which branch points begin to appear. Then Equation 13 can be used to calculate z_0 for the 11 turbulence cases. Then the propagation distance is shifted by z_0. To see the magnitude of this effect, the data in Figure 3 is replotted in Figure 4 with the plot's domain recast into $z - z_0$.

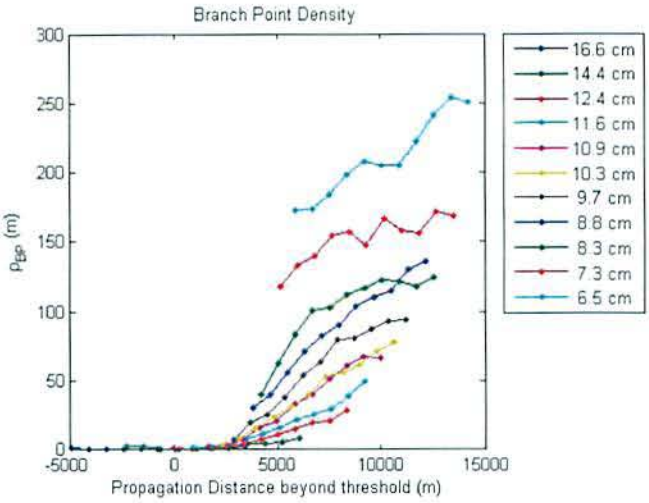

Figure 4. *Branch point density from single phase wheel data for selected turbulence strengths. For each curve, the turbulence strength, given by r_0, is held constant while the propagation distance is varied using the optical trombone. Branch point density vs propagation distance with ρ_{BP} plotted versus scaled propagation distance $(z - z_0)$.*

This form clearly demonstrates that branch point density has a stronger dependence on turbulence strength than propagation distance.

4.4 Normalizing by r_0

The iso-r_0 density curves appear to have a regular separation. Through experimentation, we have found that multiplication of the density by $r_0^{11/3}$ yields an interesting result when plotted against the transformed propagation distance, see Figure 5. The variation in atmospheric strength between the density curves is accounted for by this function of r_0. The combination of the transformation of the propagation distance by z_0 and the normalization by the function $r_0^{11/3}$ appears to have collapsed the data into predominately a single curve. The results depicted in Figure 5 demonstrate that the branch point distribution is dependent on the strength of the turbulence and the distance of propagation with no other factors playing a strong role. This implies that the density is a predictable parameter of the atmospheric turbulence and should be reducable to a functional relationship similar to the other parameters used in quantifying atmospheric conditions.

At higher turbulence strengths and greater propagation distances the density deviates from the dominate trend suggesting a saturation effect at work in the branch point distribution. That the saturation effects appear well below the maximum density that the WFS could theoretically measure (roughly $6000 pts/m^2$) indicates that this is some self imposed constraint within the turbulence.

4.5 Empirical Algebraic Form for Branch Point Density

With such a well defined curve it is possible to use this information to build an empirical formula for the branch point density as a function of r_0 and propagation distance, z. The value of $\rho_{BP}\ r_0^{11/3}$ appears to only be a function of the propagation distance beyond the branch point threshold, z_0. Examining the curve $\rho_{BP}\ r_0^{11/3}$ versus $z - z_0$ in log-log space reveals a functional form proportional to $z^{11/6}$.

Incorporating this dependence into an empirical relationship yields

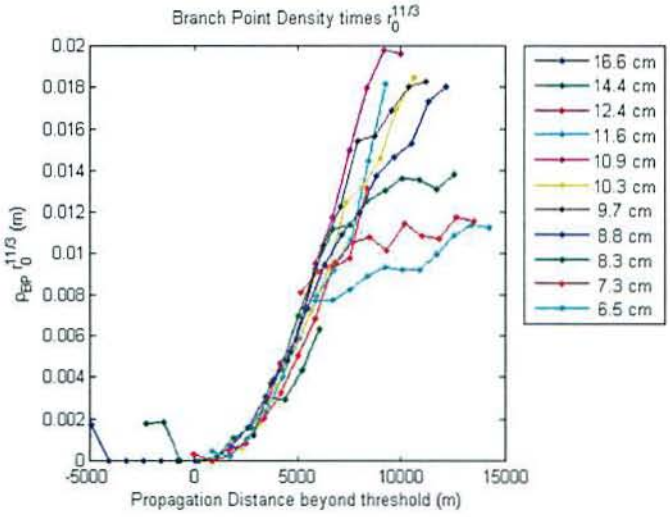

Figure 5. *Branch point density from single phase wheel data for selected turbulence strengths. For each curve, the turbulence strength, given by r_0, is held constant while the propagation distance is varied using the optical trombone. Branch point density vs propagation distance with ρ_{BP} normalized by $r_0^{11/3}$ plotted versus scaled propagation distance $(z - z_0)$*

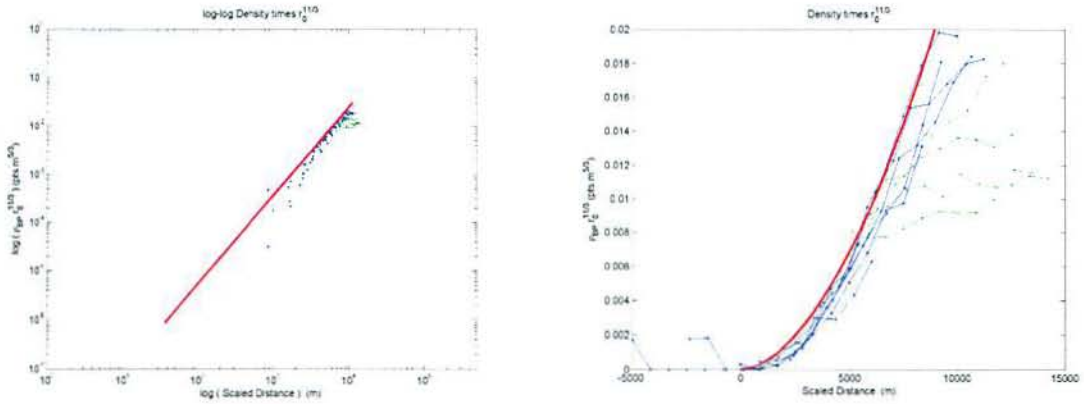

(a) (b)

Figure 6. *Estimating the functional dependence of $\rho_{BP} r_0^{11/3}$ on the scaled propagation distance, $z - z_0$. (a) The density data in log − log space shown as green and blue dots. The green dots indicate those points that appear to show signs of "saturating" away from the general behavior of the main curves. Overlaid with a red line representing a best linear fit that demonstrates the $11/6^{th}$ power dependence. (b) The same $11/6^{th}$ functional form overlaid on the data plot.*

$$\rho_{BP_{emp}} = C_\rho k_0^{-5/6} r_0^{-11/3} z_0^{-1} (z - z_0)^{11/6} \tag{14}$$

with k_0 the wave number and C_ρ as a scaling constant. Also, an additional z_0 term was added to account for scaling and balancing the units between the left and right hand sides of the equation.

This function is over-plotted on the measured branch point densities for the data sets from Table 1 in Figure 7. C_ρ in Equation 14 is set to 0.747, which was determined through a optimization algorithm to fit each curve using a least squares style norm and then optimizing the result across all of the curves simultaneously. Interestingly, this experimentally derived constant for C_ρ is almost exactly the inverse of the constant in the Rytov equation, 0.5631(2.88/2.91), or 0.7511. In Figure 7 each subplot displays the density versus propagation distance. The turbulence strength increases from left to right and from top to bottom. The branch point densities for each configuration are plotted against the unscaled propagation distance in blue. The green curve represents what is predicted from Equation 14. The red circles indicate points where the Rytov value was above 0.4. As can be seen, for $\sigma_\chi^2 < 0.4$, Equation 14 gives reasonable results. However, above $\sigma_\chi^2 \approx 0.4$, it fails and this is approximately where Sasiela[15] notes that the Rytov approximation fails mathematically.

5. DISCUSSION

The inclusion of the optical trombone to the standard ATS configuration provided a useful tool for the examination of the behavior of branch points within the turbulence generated by the simulator. The experiment provided significant data into the behavior of branch points within the ASALT lab optical systems and has helped spawn a new thread of research within the labs regarding the aggregate behavior of branch points in our experiments. This work is being continued along several avenues and will be the material for a number of future papers already in progress.

Unfortunately, for the original purpose of this research, the discovery of saturation in the branch point density limits the use of this parameter as a means of verifying the simulated turbulence from open loop data. Further, that the saturation begins to separate the measured densities from the empirically derived equation at the same Rytov value, ≈ 0.4, that the scintillation index fails, the branch point density alone offers no additional calibration of the ATS than scintillation measurements already provide.

Finally the work here is valid only for a single turbulence layer modeled in the ASALT laboratory. Further work is necessary to determine the validity of these predictions in a larger scope.

6. ACKNOWLEDGMENTS

We would like to express our gratitude to the Air Force Office of Scientific Research for their support in funding this research.

REFERENCES

1. S. V. Mantravadi, T. A. Rhoadarmer, and R. S. Glas, "Simple laboratory system for generating well-controlled atmospheric-like turbulence," in *Advanced Wavefront Control: Methods, Devices, and Applications II*, M. K. Giles, J. D. Gonglewshi, and R. A. Carerras, eds., *Presented at the Society of Photo-Optical Instrumentation Engineers (SPIE) Conference* **5553**, pp. 290–300, Oct. 2004.
2. D. L. Fried and J. L. Vaughn, "Branch cuts in the phase function," *Applied Optics* **31**, pp. 2865–2882, May 1992.
3. D. L. Fried, "Branch point problem in adaptive optics," *Journal of the Optical Society of America* **15**, pp. 2759–2768, October 1998.
4. I. Freund and M. Wilkinson, "Critical-point screening in random wave fields," *Journal of the Optical Society of America* **15**, pp. 2892–2902, November 1998.
5. D. L. Fried, "Using the hidden phase formulation in wave front reconstruction," Tech Note TN-100, David Fried, August 1999.

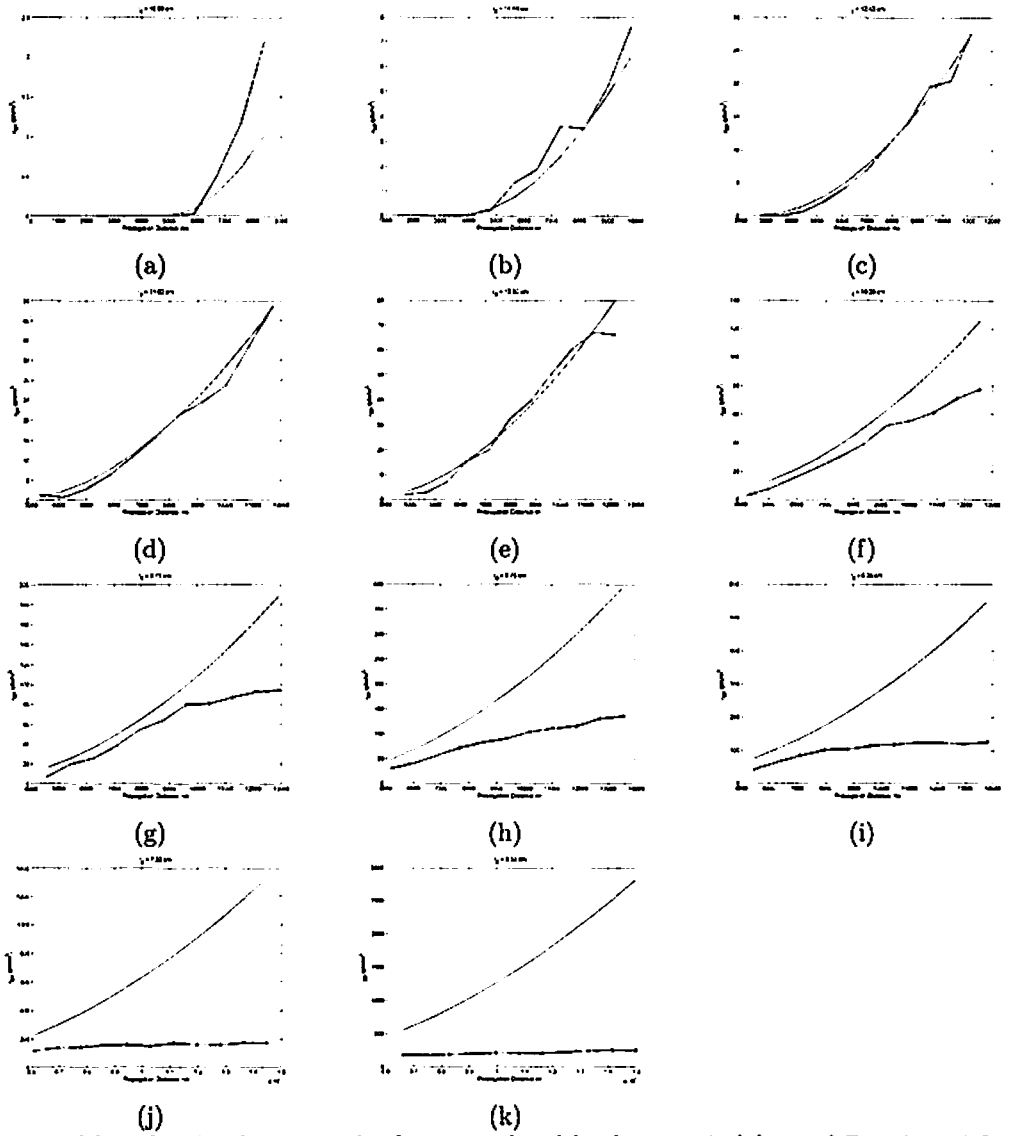

Figure 7. *Measured branch point density vs the density predicted by the empirical form of Equation 14 for each of the tested r_0's. In each case the measured ρ_{BP} is plotted in blue while the empirically predicted value is plotted as a green curve. The blue dots circled in red indicate the points whose configuration was set for a Rytov value of 0.4 or greater. (a) $r_0 = 16.6cm$ (b) $r_0 = 14.4cm$ (c) $r_0 = 12.4cm$ (d) $r_0 = 11.6cm$ (e) $r_0 = 10.9cm$ (f) $r_0 = 10.3cm$ (g) $r_0 = 9.7cm$ (h) $r_0 = 8.8cm$ (i) $r_0 = 8.3cm$ (j) $r_0 = 7.3cm$ (k) $r_0 = 6.5cm$.*

6. D. L. Fried, "Adaptic optics wave function reconstruction and phase unwrapping when branch points are present," *Optics Communications* , pp. 43–72, December 2001.
7. T. J. Brennan, "Estimation of atmospheric parameters from the slope discrepancy," Tech. Rep. TR-1609, The Optical Sciences Company, Anaheim, CA, April 2003.
8. D. L. Fried, "Crypto branch points: a problem in phase unwrapping," Tech Note TN-190, David Fried, February 2005.
9. T. M. Venema and J. D. Schmidt, "Optical phase unwrapping in the presence of branch points," *Optics Express* **16**, pp. 6985–6998, May 2008.
10. D. J. Sanchez, D. W. Oesch, C. M. Tewksbury-Christle, and P. R. Kelly, "The Aggregate Behavior of Branch Points - The Creation and Evolution of Branch Points," in *2009 SPIE Annual Conference*, R. Carerras, T. Rhoadharmer, and D. Dayton, eds., SPIE, 2009. Accepted for publication.
11. D. W. Oesch, D. J. Sanchez, P. R. Kelly, K. P. Vitayaudom, C. Tewksbury-Christle, J. Smith, and N. E. Glauvitz, "The Aggregate Behavior of Branch Points: An Overview of Research in the ASALT lab," in *2009 DEPS Annual Conference*, D. Herrick, ed., Directed Energy Professional Society, 2009.
12. C. M. Tewksbury-Christle, D. W. Oesch, D. J. Sanchez, and P. R. Kelly, "The Aggregate Behavior of Branch Points - The Use of Branch Point Pairing to Generate a Hidden Phase for Closed-Loop AO," in *2009 SPIE Annual Conference*, R. Carerras, T. Rhoadharmer, and D. Dayton, eds., SPIE, 2009. Accepted for publication.
13. D. W. Oesch, D. J. Sanchez, C. M. Tewksbury-Christle, and P. R. Kelly, "The Aggregate Behavior of Branch Points - Branch Point Density as a Characteristic of an Atmospheric Turbulence Simulator," in *2009 SPIE Annual Conference*, R. Carerras, T. Rhoadharmer, and D. Dayton, eds., SPIE, 2009. Accepted for publication.
14. V. V. Voitsekhovich, D. Kouznetsov, and D. K. Morozov, "Density of turbulence-induced phase dislocations," *Applied Optics* **37**, pp. 4525–4535, July 1998.
15. R. J. Sasiela, *Electromagnetic Wave Propagation in Turbulence: Evaluation and Application of Mellin Transforms*, SPIE Press, Bellingham, Wa, USA, 2 ed., 2007.
16. D. Washburn and R. R. Butts, "Does the detailed turbulence profile matter?." Completed while working for the Air Force Research Laboratory.

DISTRIBUTION LIST

DTIC/OCP
8725 John J. Kingman Rd, Suite 0944
Ft Belvoir, VA 22060-6218 1 cy

AFRL/RVIL
Kirtland AFB, NM 87117-5776 2 cy

Patrick Kelly
Official Record Copy
AFRL/RDSAE 1 cy